This is an *Accepted Manuscript*, which has been through the Royal Society of Chemistry peer review process and has been accepted for publication.

Accepted Manuscripts are published online shortly after acceptance, before technical editing, formatting and proof reading. Using this free service, authors can make their results available to the community, in citable form, before we publish the edited article. We will replace this *Accepted Manuscript* with the edited and formatted *Advance Article* as soon as it is available.

You can find more information about *Accepted Manuscripts* in the **Information for Authors**.

Please note that technical editing may introduce minor changes to the text and/or graphics, which may alter content. The journal's standard **Terms & Conditions** and the **Ethical guidelines** still apply. In no event shall the Royal Society of Chemistry be held responsible for any errors or omissions in this *Accepted Manuscript* or any consequences arising from the use of any information it contains.

Proton Trapping in Y and Sn Co-Doped BaZrO$_3$

James A. Dawson* and Isao Tanaka

Department of Materials Science and Engineering, Kyoto University, Sakyo, Kyoto, 606-8501, Japan

ABSTRACT

Recent experimental and computational works have shown that Y and Sn co-doped BaZrO$_3$ (BZSY) exhibits superior hydration ability and improved power output performance to that of the traditional solid oxide fuel cell (SOFC) electrolyte, Y-doped BaZrO$_3$ (BZY). BZSY is also chemically stable in both H$_2$O and CO$_2$ atmospheres and is thought to have great potential as a future electrolyte material in proton-conducting SOFCs. Herein, we report the use of potential-based calculations in the assessment of dopant-proton trapping in this exciting new material. We use a genetic algorithm to find the lowest energy BZSY configuration and then proceed to locate the lowest energy proton doping sites. Calculations of the binding energies between the proton and a range of trivalent dopants, commonly used for these kinds of electrolyte, reveal its dependence on local chemical structure and can range from weak values to values far in excess of previous computational and experimental results for BZY. Our results strongly indicate that excessive doping of BZSY, either with Y or other aliovalent dopants, maybe detrimental to performance as the concentration of potentially trapped proton sites increases.

Electronic mail: doson5888@gmail.com
Telephone number: +81-75-753-5435

1

1. Introduction

While protonic conduction in perovskites has received considerable attention for a number of electrochemical applications[1-4], their primary application is for fuel cells. The main advantage of these materials is their lower operating temperatures (400-700 °C), when compared to traditional oxygen ion conductors like yttria-stabilised zirconia (YSZ) (> 900 °C)[1,2,5]. Proton transport in these materials is, therefore, usually easier and the activation energy is lower. One of the most important and well studied proton conducting perovskites is acceptor-doped $BaZrO_3$. This material also has the additional advantages of low electronic conductivity, highly desirable for fuel cell applications, and excellent chemical and mechanical stability[1,2]. Despite the importance of these materials, many aspects of their defect chemistry remain unclear and this is especially true for the numerous variations of acceptor-doped materials.

When substitution at the B-site tetravalent cation with a trivalent dopant cation occurs, the basicity of the system increases and oxygen vacancies are formed in order to charge compensate. This makes the material more reactive to water and allows the following hydration reaction to occur:

$$H_2O + O_O^x + V_O^{\bullet\bullet} \rightarrow 2OH_O^{\bullet}. \tag{1}$$
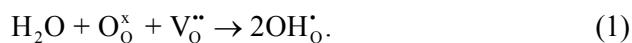
Protonic conduction in solid state materials is attributed to the Grotthuss mechanism[6,7] where protons 'hop' between neighbouring oxygen ions by thermal activation. There are generally three possible motions of protons in a perovskite: (1) reorientation – the proton rotates by 90° around the B-O-B axis while still remaining bonded to the oxygen ion; (2) intraoctahedral hopping – the proton moves from one oxygen ion to another oxygen ion of the same octahedra; (3) interoctahedral hopping – the proton moves from one oxygen ion to another oxygen ion of a different octahedra. One important influence, crucial to such proton transport, is that of dopant-proton trapping which results from several factors including the interaction

between positively charged protons and negatively charged dopants and local strain effects[8]. At high hydration and dopant concentrations, such trapping effects can seriously hinder long-range proton transport.

To the best of our knowledge, there are only two previous studies of Y and Sn co-doped $BaZrO_3$ (BZSY) as an electrolyte for SOFC applications, one experimental[2] and the other, our own previous computational study[9]. In the experimental study, XPS spectra and TGA analysis both confirm that BZSY has greater hydration ability than BZY. The peak in the XPS spectrum for the O 1s core level shifts to the lower binding energy which suggests increased basicity[10] and therefore favouring of the formation of protonic defects[11,12]. Clearly, increased proton concentration is important for increasing proton-conductivity (although it is important to note that this is not always the case) and this is confirmed by impedance spectra which show an improved total electrical conductivity for BZSY compared to BZY, albeit with a marginally higher activation energy (0.38 eV for BZSY compared to 0.37 eV for BZY). Practical testing of BZSY has confirmed the highest ever reported power performance for a proton-conducting SOFC with a $BaZrO_3$-based electrolyte. Tolerance to H_2O and CO_2 atmospheres has also been shown to be excellent. Density functional theory (DFT) calculations[9] confirmed excellent hydration ability with values larger than any previously calculated for an acceptor-doped BZY electrolyte. Low energy proton migration pathways were also found and the synergy between the Sn and Y dopants in producing the excellent performance of the material was illustrated.

There have been several experimental and computational studies of proton-trapping in acceptor-doped BZY and $BaZrO_3$, but our study is the first for BZSY. Yamazaki et $al.$[8] combined thermogravimetric and a.c. impedance measurements to obtain a value of 29 $kJmol^{-1}$ for the proton-dopant association energy in BZY. This value was in good agreement with the value obtained from Neutron-Spin-Echo (NSE) experiments which also illustrated

3

how the proton diffuses slower when in the vicinity of a Y dopant ion[13]. Several of our own studies have also confirmed similar results for BZSY[9] and ZrO_2/YSZ[14-16]. Stokes and Islam[1] used potential-based calculations to simulate proton doping of $BaZrO_3$. They calculated the attraction between the proton and a range of trivalent dopants typically used in electrolytes. For all dopants tested, an attraction was found with values ranging from ~ -0.17 eV for Ga (a large dopant) to ∼ -0.78 eV for Sc (a smaller dopant). Similar values were also obtained using DFT calculations[17].

In this study, we use potential-based calculations to, for the first time, assess dopant-proton trapping in this exciting new material. Previous studies have demonstrated the strong potential of BZSY for use as an electrolyte, however, it is not yet known what the influence proton-trapping has on long-range proton transport in the material. For these types of calculation, it is common for authors to consider only a simple, undoped unit cell and then add one or two defects. We consider thousands of configurations with several hundreds of ions each and use a genetic algorithm to find the lowest energy configuration among them. By considering a simulation cell with several hundreds of ions, we are able to consider far more proton and dopant sites, and therefore gain a far greater understanding into proton trapping in this material.

2. Methodology

The results presented here are based on well established simulation techniques based on the Born model for ionic solids. The energy of the system is modelled from contributions of the long-range and short-range forces with respect to the atomic positions in the lattice. The long-range interactions are Coulombic and the short-range repulsive interactions are represented by Buckingham potentials:

$$V_{ij}(r) = \sum_{i \neq j}^{n} A \exp(-r_{ij} / \rho) - \frac{C}{r_{ij}^6} \qquad (2)$$

where the symbols have their usual meanings. All the ions are assumed to be fully ionic and therefore have formal charges. A cutoff of 12 Å was applied to all of the potentials. In this work, we use a proven potential model previously applied to the calculation of proton doping and proton-defect binding in $BaZrO_3$[1]. This model has been shown to excellently reproduce the perovskite structure. For the Sn-O and Y-O interactions, we use potentials developed by Lewis and Catlow[18]. All dopant-oxygen interactions were also taken from Lewis and Catlow with the exception of the In-O potential which was taken from Minervini *et al.*[19]. All these potentials use the Dick-Overhauser shell model[20] to account for polarizability. However, in our simulations, the use of the shell model caused serious instabilities during optimization as some core-shell distances exceeded the cutoff. Such an issue is not uncommon when large, complicated systems with many defects are considered[21,22]. As a result, we have decided not to use the shell model in our simulations.

For the interactions of the proton, we use an attractive Morse potential. This potential was fitted using *ab initio* cluster calculations[23] to describe the O-H interaction. A Buckingham potential is also used to describe the interactions between the OH group and the surrounding lattice[24]. The Morse potential is written as:

$$V(r) = D\{1 - \exp[-\beta(-r / r_0)]\}^2 \qquad (3)$$

where D, β and r_0 are the parameters obtained from *ab initio* quantum mechanical cluster calculations with a point charge representation of the surrounding lattice[23]. The OH group is given the correct overall charge of -1 by distributing the dipole across both ions with an oxygen charge of -1.4263 and a hydrogen charge of +0.4263. This method has been

successfully used to model protonic defect chemistry in a range of materials including perovskites[1,25,26] and ZrO_2/YSZ[14-16].

All defect energetics calculations are performed using the Mott-Littleton approximation[27]. In this method the defects are simulated at the infinitely dilute concentration limit. The lattice surrounding the defect is divided into two spherical regions; an inner region and outer region. In the inner region the interactions are calculated explicitly and ions are relaxed to positions of zero force. In the outer region, where the interactions are weaker, the polarisation energy and ionic positions are approximated using a dielectric continuum method. To ensure the inner region is properly bedded in the crystal the interactions between ions of the inner region and the ions of the outer regions are calculated explicitly. Comprehensive reviews of the methodologies briefly described here are available elsewhere[28,29]. All the calculations in this work were completed using the General Utility Lattice Program (GULP)[30].

In order to find the lowest energy BZSY configuration, we used a genetic algorithm (GA) that has been previously used for identifying lowest energy configurations of doped $BaTiO_3$[31-33]. We started with ten random BZSY configurations constructed using a random number generator. The atomic coordinates of each Zr ion were assigned a random number and then sorted numerically. Zr ions placed first in the list were then replaced with the appropriate number of Sn and Y ions to produce unique, random configurations. A similar procedure was adopted for the introduction of the oxygen vacancies. These starting configurations are fully optimized and then ten more configurations are created by mixing the previous ten configurations together. This mixing procedure is governed by the energy of the configurations so that the more stable configurations are more likely to be used. This process was repeated for 20 cycles until only the lowest energy configurations remain. The whole GA procedure was repeated several times to ensure that sufficient unique configurations had been sampled. More details on this GA approach are available in our studies of doped $BaTiO_3$.

6

For our calculations we use a BZSY supercell consisting of $4 \times 4 \times 3$ perovskite unit cells which contains 235 ions and is equivalent to $Ba_{48}Zr_{33}Sn_5Y_{10}O_{139}$ ($BaZr_{0.69}Sn_{0.10}Y_{0.21}O_{3-\delta}$). This defect concentration was chosen to achieve the best possible comparison with experiment where $BaZr_{0.7}Sn_{0.1}Y_{0.2}O_{3-\delta}$ was synthesized[2]. All ions are treated in their formal oxidation states, as confirmed by experiment[2]. Figure 1 shows the optimized, lowest energy BZSY configuration used for all the calculations in this work. Its calculated lattice parameter is compared to the experimental value and the value obtained from previous DFT calculations[9] in Table 1. The agreement with the experimental value is excellent and even improves upon the value obtained from DFT calculations.
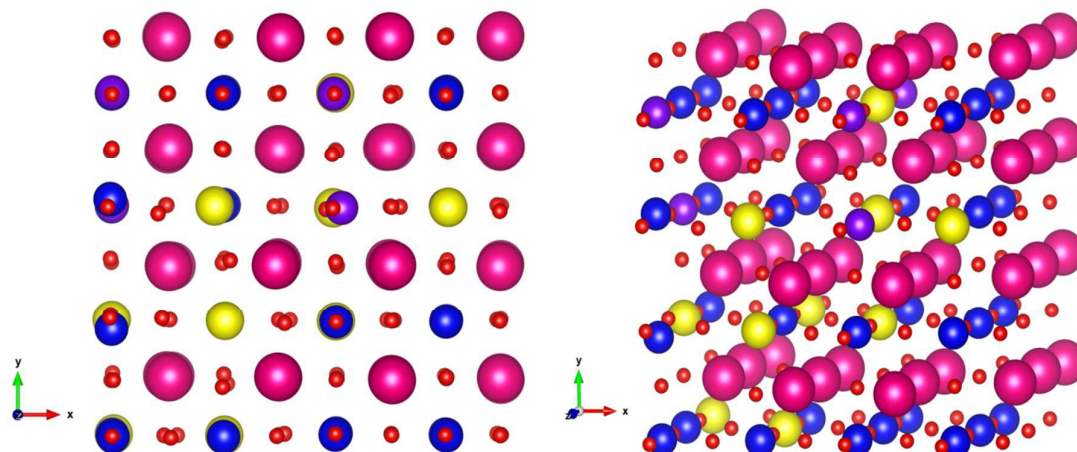
Fig 1. Optimized, lowest energy unhydrated BZSY supercell. Pink spheres represent Ba ions, blue spheres are Zr ions, yellow spheres are Y ions, purple spheres are Sn ions and red spheres are oxygen ions. This colour scheme is consistent throughout the manuscript.

Table 1: Calculated and experimental lattice parameters for BZSY.

	a (Å)		
	This work	Experiment[1]	GGA[9]
BZSY	4.230	4.198	4.271 ($\pm$0.01)

3. Results and Discussion

3.1. Proton site stability

Before considering proton-dopant interactions, we must locate the lowest energy proton doping sites. This was also previously studied using DFT calculations[9] and it was found that protons are most energetically stable when the oxygen ion they are bonded to neighbours a Y ion, as a result of Coulombic attraction. Proton sites were also found to be least energetically stable when in the vicinity of a Sn ion due to Coulombic repulsion. On this basis, we only consider proton sites that are close to at least one Y ion. In the perovskite structure, the oxygen bound hydrogen interstitials align along the [100]-type directions in the interoctahedral space. There are potentially four positions for the proton to occupy per oxygen ion, as illustrated for BZY in Figure 2. In an undoped structure all these positions are equivalent; however when dopants are introduced to the system the situation becomes more complex. There are ten Y ions in the BZSY supercell and for each of these Y ions, we locate the closest oxygen ion and then use these ions to locate the lowest energy proton doping sites. Each of these doping sites is unique and their local chemical structure can differ dramatically. By finding the most stable proton doping sites at these unique sites and then calculating the proton-dopant interactions for each site, we can gain a far greater insight into the influence of these interactions than is possible for an ideal, simple unit cell.
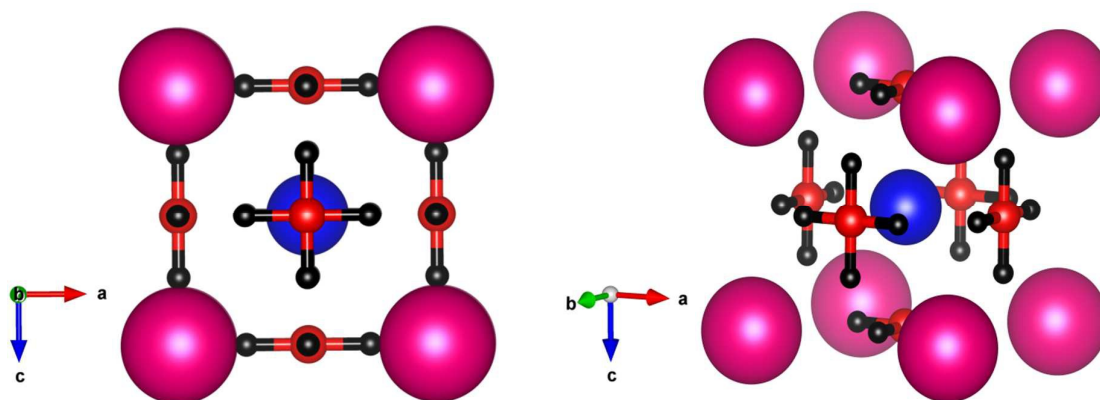
Fig. 2. Illustrations of the 4 possible proton sites for each oxygen ion in BZY. The colour scheme is the same as defined in Figure 1 with the addition of black spheres for protons.

The lowest energy proton positions in the vicinity of each Y ion are given in Figure 3. While in an ideal structure, like that of Fig. 2, the proton positions are clearly defined, in a solid solution with a high concentration of defects, the optimal position of the proton can vary significantly depending on the local chemical environment. Each of the ten local configurations displayed in Fig. 3 have very different structures, some with high concentrations of Y or Sn and some with oxygen vacancies in close proximity. Some protons, such as those in configurations 3, 6 and 8, align towards Y ions as observed for BZSY previously[9]. However, others cause significant displacement of the attached oxygen ion and appear to bind with other nearby oxygen ions (configurations 1, 2, 7 and 10). Configuration 2 shows the distortion an oxygen vacancy causes to the octahedra of the nearby Y ion. O-H bonds also tend to point away from nearby Sn ions because of the Coulombic repulsion between them, as also calculated by DFT calculations[9].
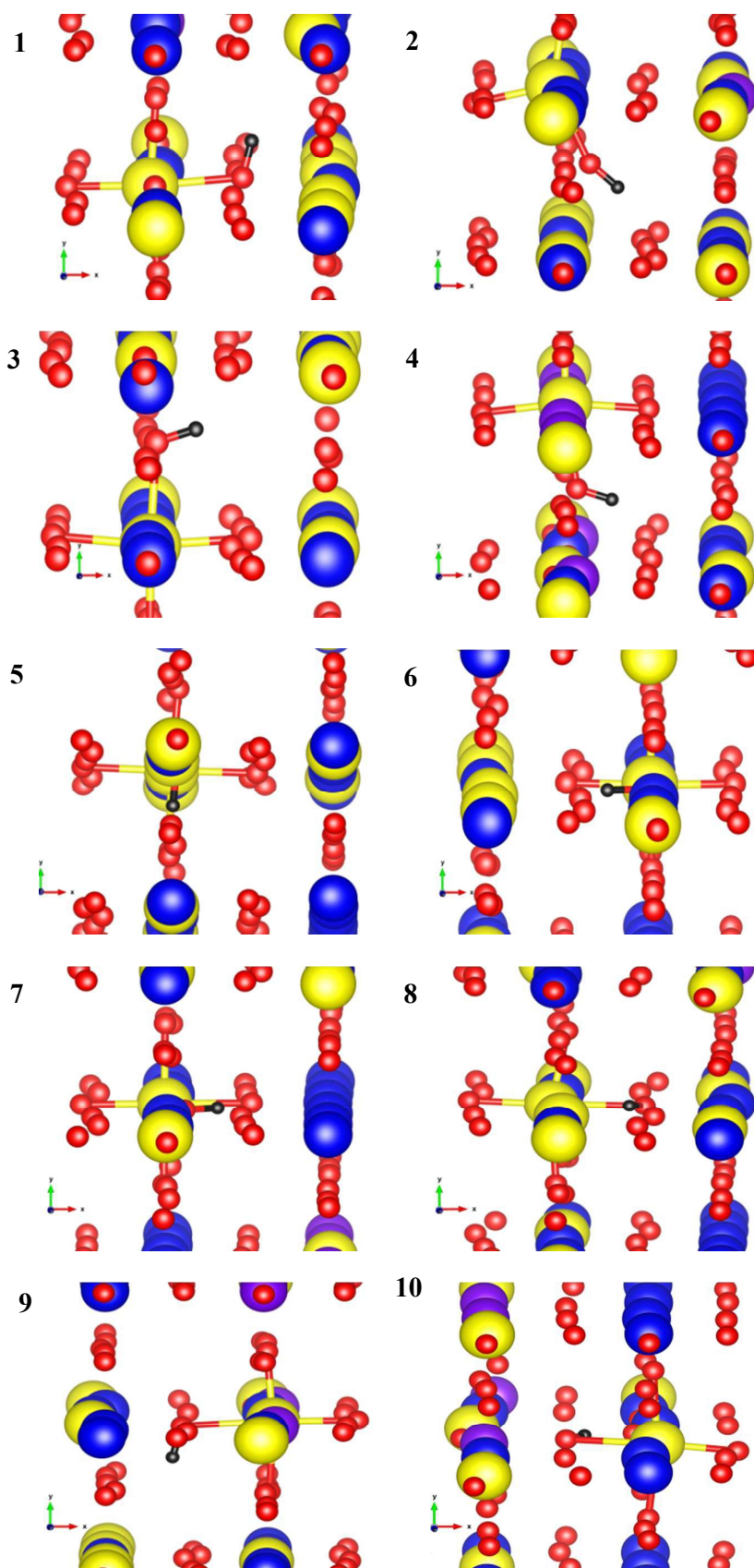
Fig. 3. Lowest energy proton positions for each of the ten oxygen ions considered in the BZSY supercell. Ba ions have been omitted for clarity and the bonds of the Y ion closest to the OH species are also displayed.

3.2. Proton-dopant interactions

Although there has been debate in recent years over the existence of significant trapping effects in hydrated perovskites, many recent studies, both computational and experimental, clearly suggest the existence of trapped protons in $BaZrO_3$/BZY[1,8,13,17]. Therefore, in order for these protons to achieve long-range transport, an additional energy barrier must be overcome. By placing an additional aliovalent dopant ion at the Zr ion closest to the proton in each configuration, we can calculate the binding energy between the positively charged proton and negatively charged dopant site. We can also assess the effect of the additional dopant ion on the orientation of the O-H bond in each of the ten configurations. In this study, we use Sc, In, Yb, Y and Gd as the dopants as they are typically added to these kinds of material. The binding energy (E_{bind}) between oppositely charged defects is defined as the difference between the total energy of the isolated defects and the energy when the same defects are simulated together in a cluster:

$$E_{bind} = E(X) + E(Y) - E(XY) \qquad (4)$$

where a negative value implies a stable cluster and binding behaviour.

Plots of the binding energies for each of the ten configurations are displayed in Fig. 4. Perhaps the most important feature of these results is that with the exception of configuration 10, all the binding energies are negative which suggests the existence of trapping effects in BZSY. When binding energies are calculated for proton-dopant pairs in ideal $BaZrO_3$ or BZY

unit cells[1,7], there is normally a simple relationship where binding energy increases with decreasing dopant ionic radius as a result of simple Coulombic arguments. Our results show that this is clearly not always the case for a more "realistic" solid solution supercell.
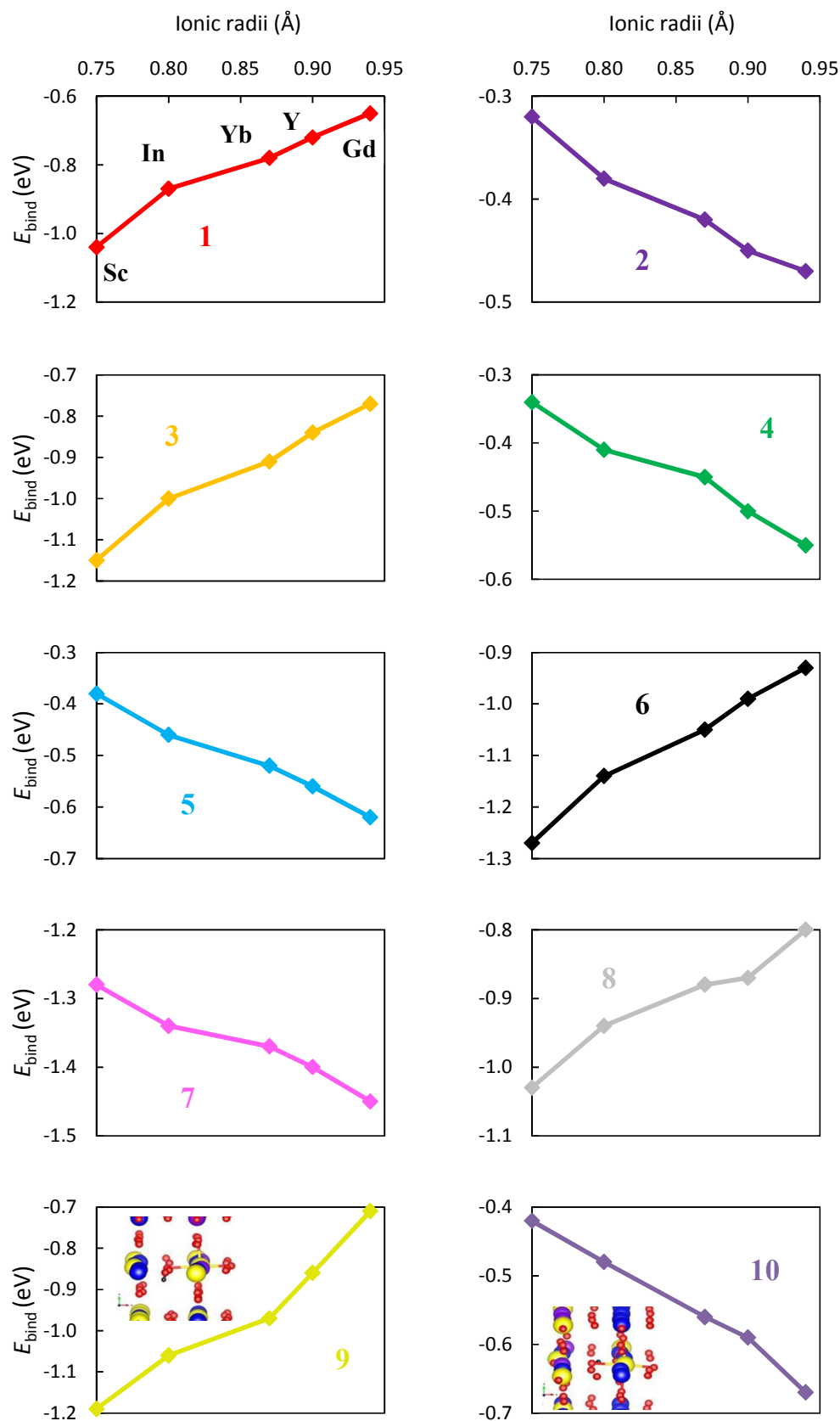
Fig. 4. Proton-dopant binding energies for a range of aliovalent dopants at ten unique sites (as determined in Fig. 3) in BZSY.

The binding energies for all configurations obey one of two trends. Configurations 1, 3, 6, 8 and 9 exhibit the expected trend of increasing binding energies with decreasing dopant ionic radius, while configurations 2, 4, 5, 7 and 10 display entirely opposing behaviour. The former configurations contain proton-dopant pairs that are nearest neighbours and therefore the binding energies are strong. Configurations 2, 4, 5 and 10 contain proton-dopant pairs with greater separation and therefore generally weaker binding energies. While it is clear why interatomic distance plays a crucial role in determining the binding energies in these configurations, it is not clear why larger dopant ions produce stronger binding energies than smaller ones when they are not nearest neighbours to the proton.

The calculated proton-dopant interatomic distances are given in Table 2. Analysis of these distances in these optimized configurations reveals that, as expected, small dopant ions like Sc are closer to the proton than large ions like Gd. However, there is a clear difference between configurations with the proton and dopant as nearest neighbours and those where the distance between the proton and dopant is greater. For configurations 1, 3, 6, 8 and 9, all the proton-dopant distances are shorter than the distance between the original Zr ion and the proton which explains the strong binding energies of these configurations. For the other configurations, generally, the proton-dopant distances are longer and therefore the binding energies are weaker. The exception to this is configuration 7 which has longer proton-dopant distances and strong binding energies. This is discussed in more detail below.

The fact that longer proton-dopant interatomic distances produce weaker binding energies does not, however, explain why larger dopant ions have stronger binding energies than smaller ions in some of the configurations. A possible explanation comes from analysis of the local structure surrounding the dopant ion. Smaller dopant ions have a tendency to draw in surrounding oxygen ions and slightly move them away from the proton, thus decreasing the electrostatic attraction between them and therefore the energetic stability of the proton. This

effect is not as strong for larger dopant ions which may partially explain why the binding

energy is stronger between large dopant ions and protons when the interatomic distance

between them is further than nearest neighbour distances. We attempt to illustrate this effect

for configuration 2 in Fig. 5. This reinforces the importance of considering defect

configurations different to those in an ideal cell and also the importance of binding beyond

nearest neighbour defects.

Table 2: Calculated dopant-proton (M-H) distances for each dopant and configuration tested.

Ion	Ionic radius (Å)[34]	M-H (Å)									
		1	**2**	**3**	**4**	**5**	**6**	**7**	**8**	**9**	**10**
Zr	0.72	2.44	3.26	2.38	3.38	3.71	2.32	2.90	2.85	2.42	3.50
Sc	0.75	2.24	3.32	2.21	3.53	3.72	2.18	2.81	2.50	2.24	3.55
In	0.80	2.30	3.35	2.25	3.54	3.75	2.19	2.88	2.57	2.29	3.59
Yb	0.87	2.33	3.35	2.28	3.55	3.77	2.21	2.94	2.62	2.33	3.61
Y	0.90	2.34	3.35	2.29	3.55	3.78	2.22	2.96	2.63	2.35	3.63
Gd	0.94	2.40	3.37	2.33	3.57	3.81	2.26	3.02	2.67	2.39	3.65

(a) (b)
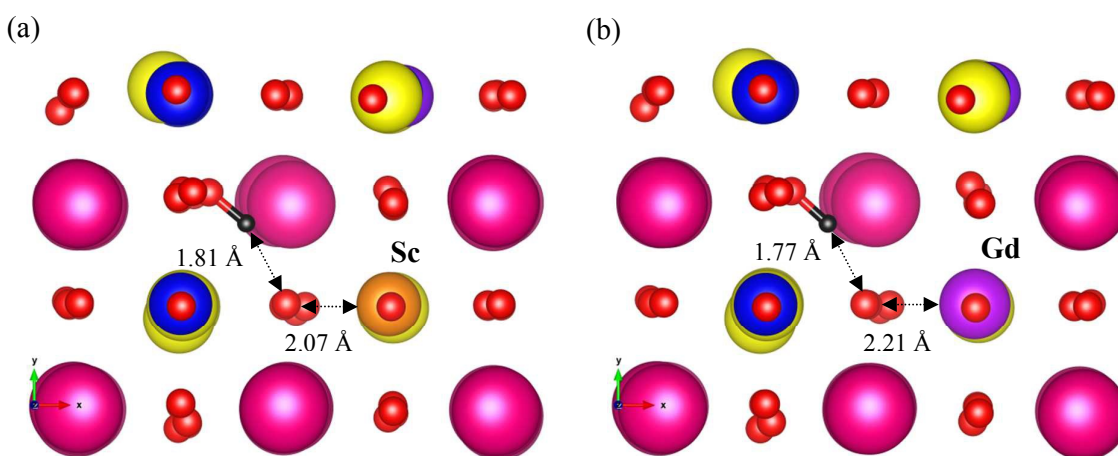
Fig. 5. Binding between a proton and (a) a Sc dopant ion and (b) a Gd dopant ion in configuration 2.

The binding behaviour displayed in configurations 7 is very different to that of the other configurations. This configuration shows the strongest binding energies for all configurations, however the trend with dopant size is opposite to what would be expected for when the dopant and proton are nearest neighbours. Furthermore, as Table 2 shows, with the exception of Sc, all proton-dopant distances are larger than the starting Zr-H distance. As previously discussed, this is a feature of a configuration where the proton and dopant are not nearest neighbours. In fact, overall the results for this configuration appear to be a combination of those observed for configurations with proton-dopant nearest neighbours and configurations with the proton and dopant more separated. Fig. 3 shows that the proton in configuration 7 is in an unusual position and is actually almost bridged between two oxygen ions. In this configuration, the proton is effectively prevented from getting closer to the dopant ion because of their positions. A similar effect was also calculated for Gd-doped $BaZrO_3$[1]. For larger dopant ions like Gd, the distance between the proton and the second bridging oxygen ion is at a minimum, thus maximising the interaction between the two ions and causing the

strong binding energy. This example illustrates how even for nearest neighbours, the trend is not always as simple as increasing binding energy with decreasing dopant size.

Our results for configurations with the dopant ion substituted at a site not directly neighbouring the proton are in good agreement with calculations using the same potential model for $BaZrO_3$[1]. Stokes and Islam calculated values between ~ -0.17 eV and -0.78 eV for the same dopants used in this work. Some of the values calculated for BZSY are significantly stronger than those calculated for $BaZrO_3$ which suggests a potential barrier for long-range proton transport in the material. This is further supported by the much weaker binding energies calculated for BZY by Björketun *et al.*[17] of between -0.14 for Gd and -0.23 eV for Sc. The values for BZSY are also dramatically larger than those for BZY (-0.29 eV)[8] and other doped perovskite materials (-0.2 and -0.4 eV for Sc-doped $SrZrO_3$[35] and Yb-doped $SrCeO_3$[36], respectively) calculated by experiment. These results strongly indicate that excessive doping of BZSY either with Y or other aliovalent dopants maybe detrimental to performance as the concentration of potentially trapped proton sites increases. We hope that this study will encourage more experimental studies into this material so that we can further understand the nature and effects of proton trapping on its SOFC performance. In particular, combined thermogravimetric and a.c. impedance studies, such as those completed by Yamazaki *et al.*[8], are vital for providing quantitative evidence of binding in these materials. Muon spin relaxation and quasi-elastic neutron scattering have also been proven as powerful experimental techniques for assessing proton-dopant binding behaviour in these materials[35,36].

4. Conclusions

We have completed potential-based calculations of proton-dopant interactions in the new electrolyte material, Y and Sn co-doped $BaZrO_3$ (BZSY). We have used a genetic algorithm

to find the lowest energy BZSY configuration, which was then used to locate the lowest energy proton doping sites. The interaction between protons at these sites and nearby aliovalent dopants was then assessed for ten different local structures in the lowest energy BZSY supercell.

Calculations of the binding energies between the proton and a range of trivalent dopants, commonly used for these kinds of electrolyte, reveal its dependence on local chemical structure and can range from weak values to values far in excess of previous computational and experimental results for BZY. When the proton and dopant are nearest neighbours, the binding energies are strong and simple ionic size arguments dominate with the binding energy increasing with decreasing dopant ionic radius. Alternatively, when the proton and dopant are not nearest neighbours, the binding energies are far weaker and the trend is completely reversed with larger dopant ions having the stronger binding energy. Overall, our results suggest that proton trapping is an issue in BZSY and that excessive doping may hinder electrochemical performance.

By considering the lowest energy simulation cell with several hundreds of ions, we are able to consider far more proton and dopant sites, and therefore gain a far greater understanding into proton trapping in this material than would be possible for a single ideal unit cell, as used in many previous studies.

ACKNOWLEDGEMENTS

REFERENCES

(1)   Stokes, S. J.; Islam, M. S. *J. Mater. Chem*. **2010**, *20*, 6258.

(2)   Sun, W.; Liu, M.; Liu, W. *Adv. Energy Mater*. **2013**, *3*, 1041.

(3)   Iwahara, H.; Esaka, T.; Uchida, H.; Maeda, N. *Solid State Ionics* **1981**, *3*, 359.

(4)   Iwahara, H.; Uchida, H.; Tanaka, S. *Solid State Ionics* **1983**, *9*, 1021.

(5)   Kim, S.; Avila-Paredes, H. J.; Wang, S.; Chen, C. –T.; De Souza, R. A.; Martin, M.; Munir, Z. A. *Phys. Chem. Chem. Phys*. **2009**, *11*, 3035.

(6)   Agmon, N. *Chem. Phys. Lett*. **1995**, *244*, 456.

(7)   Knauth, P.; Di Vona, M. L. *Solid State Proton Conductors: Properties and Applications in Fuel Cells*, John Wiley & Sons Ltd., Chichester, West Sussex, UK **2012**.

(8)   Yamazaki, Y.; Blanc, F.; Okuyama, Y.; Buannic, L.; Lucio-Vega, J. C.; Grey, C. P.; Haile, S. M. *Nat. Mater*. **2013**, *12*, 647.

(9)   Dawson, J. A.; Miller, J. A.; Tanaka, I. *Chem. Mater*. **2015**, *27*, 901.

(10) Dimitrov, V.; Komatsu, T.; Sato, R. *J. Ceram. Soc. Jpn*. **1999**, *107*, 21.

(11) Kreuer, K. D.; Adams, S.; Munch, W.; Fuchs, A.; Klock, U.; Maier, *Solid State Ionics* **2001**, *145*, 295.

(12) Kreur, K. D. *Solid State Ionics* **1999**, *125*, 285.

(13) Karlsson, M.; Engberg, D.; Bjorketun, M. E.; Matic, A.; Wahnstrom, G.; Sundell, P. G.; Berastegui, P.; Ahmed, I.; Falus, P.; Farago, B.; Borjesson, L.; Eriksson, S. *Chem. Mater*. **2010**, *22*, 740.

(14) Dawson, J. A.; Tanaka, *J. Mater. Chem. A* **2014**, *2*, 1400.

(15) Dawson, J. A.; Chen, H.; Tanaka, I. *Phys. Chem. Chem. Phys*. **2014**, *16*, 4814.

(16) Dawson, J. A.; Tanaka, I. *Langmuir* **2014**, *30*, 10456.

(17) Björketun, M. E.; Sundell, P. G.; Wahnstrom, G. *Farad. Discuss*. **2007**, *134*, 247.

(18) Lewis, G. V.; Catlow, C. R. A. *J. Phys. C Solid State Phys*. **1985**, *18*, 1149.

(19) Minervini, L.; Zacate, M. O.; Grimes, R. W. *Solid State Ionics* **1999**, *116*, 339.

(20) Dick, B. G.; Overhauser, A. W. *Phys. Rev. B* **1958**, *112*, 90.

(21) Benedek, N. A.; Chua, A. L. S.; Elsässer, C.; Sutton, A. P.; Finnis, M. W. *Phys. Rev. B* **2008**, *78*, 064110.

(22) Dawson, J. A.; Tanaka, I. *J. Phys. Chem. C* **2014**, *118*, 25765.

(23) Saul, P.; Catlow, C. R. A. *Philos. Mag. B* **1985**, *51*, 107.

(24) Schroder, K. P.; Sauer, J.; Leslie, M.; Catlow, C. R. A.; Thomas, J. M. *Chem. Phys. Lett*. **1992**, *188*, 320.

(25) Davies, R. A.; Islam, M. S.; Gale, J. D. *Solid State Ionics* **1999**, *126*, 323.

(26) Islam, M. S.; Davies, R. A.; Fisher, C. A. J.; Chadwick, A. V. *Solid State Ionics* **2001**, *145*, 333.

(27) Mott, N. F.; Littleton, M. J. *J. Chem. Soc., Faraday Trans. 2* **1989**, *85*, 565.

(28) Harding, J. H. *Rep. Prog. Phys*. **1990**, 53, 1403.

(29) Catlow, C. R. A. *Computer Modelling in Inorganic Crystallography*, Academic Press, San Diego, California, USA **1997**.

(30) Gale, J.; Rohl, A. *Mol. Simulat*. **2003**, *29*, 291.

(31) Freeman, C. L; Dawson, J. A.; Harding, J. H.; Ben, L. B.; Sinclair, D. C. *Adv. Funct. Mater*. **2013**, *23*, 491.

(32) Freeman, C. L; Dawson, J. A.; Chen, H.; Ben, L. B.; Harding, J. H.; Morrison, F. D.; Sinclair, D. C.; West, A. R. *Adv. Funct. Mater*. **2013**, *23*, 3925.

(33) Dawson, J. A.; Harding, J. H.; Sinclair, D. C.; Freeman, C. L. *Chem. Mater*. **2014**, *26*, 6104.

(34) Shannon, R. D. *Acta. Crystallogr*. **1976**, *32*, 751.

(35) Karmonik, C.; Udovic, T. J.; Paul, R. L.; Rush, J. J.; Lind, K.; Hempelmann, K. *Solid State Ionics* **1998**, *109*, 207.

(36) Hemplemann, K.; Soetratmo, M.; Hartmann, O.; Wappling, R. *Solid State Ionics* **1998**, *107*, 269.

.

TABLE OF CONTENTS
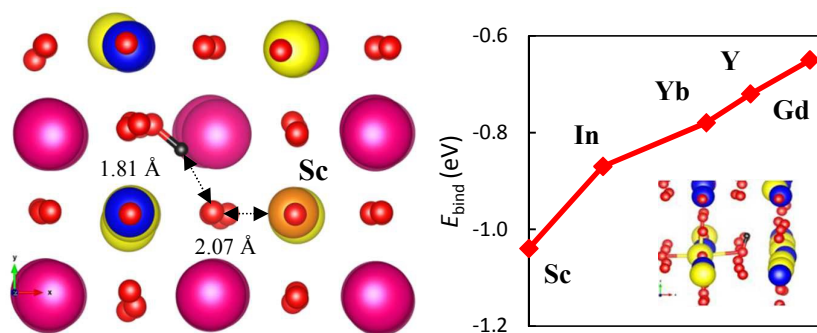
Proton-dopant interactions in the exciting new SOFC electrolyte material, Y and Sn co-doped

$BaZrO_3$, are shown to be potentially detrimental to its electrochemical performance.